EasyChair Preprint

№ 10254

Effect of Anti-fouling Coatings and Biofouling on Ship Hydrodynamic Performance

K Abhiroop and Shameem Basheer Mohammed

May 24, 2023

Effect Of Anti-Fouling Coatings and Biofouling on Ship Hydrodynamic Performance

K. Abhiroop[1] and Shameem Basheer Mohammed[2]

[1] Junior Specialist (Statutory), Lloyd's Register LLC, India
[2] Military Technological College, Sultanate of Oman
abhiroopkmadhavan@gmail.com,
shameem.mohammed@mtc.edu.om

Abstract. Bioaccumulation of the ship's submerged region would increase the hydrodynamic volume and poses a major source of carbon emissions to the atmosphere. This accumulation of marine growth on the ship's hull creates additional drag and demands more fuel consumption, predominantly leading to adverse effects on the marine ecosystem. Anti-fouling coatings are one of the primary methods adopted for a smooth hull, however, the smoothness of the hull surface is significantly dependent on the type and the chemical composition of the coatings. The present paper investigates the effect of frictional drag on a flat plate under different composition of anti-fouling coatings, and effect of various biofouling conditions on a ship's submerged hull. The numerical analysis of anti-fouling coatings on the flat plate is conducted using CFD for seven cases, viz., smooth, sandpaper and five anti-fouling cases. However, six conditions of biofouling are considered on the selected ship hull - smooth and five biofouling cases. To regenerate the appropriate roughness factor, the Colebrook-type roughness functions are used from the literature. The effect of antifouling coatings and biofouling on the flat plate and ship's hull is predicted and analyzed for various speeds of operation. The results from this work would assist to predict the remaining life and appropriate docking period, selecting the suitable antifouling coatings. This prediction would help in optimizing the fuel consumption with new CII requirements.

Keywords: CFD, Antifouling coating, Biofouling, Hull roughness, decarbonization

1 Introduction

Since most cargo is transported by sea, reducing frictional resistance would result in dramatic reductions in fuel consumption and carbon emissions. The regulations, such as the Energy Efficiency Design Index (EEDI) [1], Ship Energy Efficiency Management Plan (SEEMP) [2], and the recommended practices such as the Energy Efficiency Operational Indicator (EEOI) [3] have been implemented in recent times to limit the harmful gases that are released to the marine environment from ships. It was reported one decade ago, the quantity of CO_2 released from the shipping industry is about 870

million tons. Energy efficiency and Greenhouse Gas (GHG) regulations have thus been developed and implemented by the International Maritime Organization (IMO). Skin friction accounts for most of the total resistance (approximately 60% -70%) for most of the large commercial vessels [3]. In slow speed ships such as oil tankers, frictional resistance is nearly 80% percent of the total resistance while it is about 50% at high-speed ships such as container vessels [4].

On ship hulls, microfouling develops rapidly, and several biofilms are persistent even under the strongest antifouling coatings [5]. As a result, surface roughness, frictional resistance, and fuel consumption increase. According to [6], the increase in resistance due to micro-organism fouling is around 1-2%, whereas an accumulation of hard-shelled organisms may cause an increase in resistance of up to 40%. According to Schultz, a frigate with a speed of 15 knots required a 21% higher shaft power when slime was present [7]. Heavy calcareous fouling, on the other hand, increased shaft power by 86%, whereas slime alone resulted in a 21% increase in shaft power. It was observed that microbial slime led to an increase of 10% to 20% in frictional resistance. It has been reported that the usage of Colebrook type of wall function [8] to predict the frictional component of resistance provides a better result. It is inferred from the literature; the selection of hull coating is important to reduce the biofouling and the composition of the paint scheme affects the resistance coefficient. The objective of the present study is to validate the roughness conditions due to different anti-fouling coatings and bio-fouling stages with the published experimental data.

2 NUMERICAL METHOD

2.1 RANS Mathematical Formulation

The simulation is modelled with free surface to replicate the experimental setup given in [8]. The literature experimentally discussed the effect of anti-fouling coatings on the flat plate. In the present simulation, RANS equation is used to model computational to estimate the effect of roughness and biofouling.

2.2 Roughness Function

Prediction of roughness functions are important in estimating the frictional resistance. The submerged region that is covered with specific roughness can be predicted using the boundary layer method [12] [13]. Roughness condition on the flat plate and tanker is verified theoretically using the roughness function $\Delta U+$ and roughness Reynolds number, $k+$ [14]. For the candidate vessel, an appropriate roughness function model is fitted to the roughness function values [7] and modelled with the roughness function model in Siemens STAR-CCM+.

2.3 Geometry and Boundary Condition

The dimension of the flat plate is 1.52 m in length, 0.76 m in width, and 3.2 mm in thickness [9]. The free surface is 0.59 m from the bottom of the plate. The extension of

the domain and the boundary conditions chosen as per the ITTC recommendation [4]. A tanker (KVLCC 2) is selected for the current study, the principal particular of the vessel is available in [19]. The CFD setup for the vessel is selected within the recommendation of ITTC [4].

2.4 Meshing and Grid Independence Analysis

Since the study involves the capturing of roughness characteristics of the anti-fouling coatings and bio-fouling condition, it is important to precisely capture the boundary layer properties. Therefore, a grid independence study is carried out to analyze the solution convergence. The cell grids are generated with trimmed hexahedral cells. To capture the boundary layer, additional near wall prism layers are imposed around the plate and tanker. The number and thickness of the prism layer affects the wall Y+ function. Prism layers are selected to ensure the wall Y+, maintained at a value greater than 30 to use standard wall laws for all Reynolds numbers [11] [17].

Based on the different configuration of prism layers with the prism layer thickness 0.015m, the change in wall Y+ and the C_F value is predicted. Grid Convergence Index (GCI) is used to check the convergence of results based on Richardson extrapolation [15]. It is observed that, for more than 3 million cells, the results are minimally affected with an increase in cell density.

The frictional resistance of the tanker is computed at a design speed of 15.5 knots for different mesh configuration and the solution is converged very well with a density corresponds to 1.6 million cells. Therefore, the corresponding fine mesh configuration is selected in all subsequent computations. Fine refinements are carried out near and around the plate, tanker, and the free surface. The computational domain of the flat plate and the tanker is shown in Fig. 1 and 2 respectively.

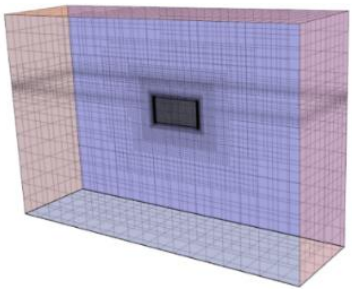

Fig. 1. Computational domain – flat plate

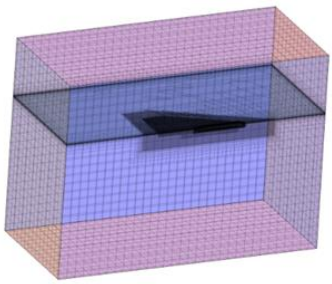

Fig. 2. Computational domain - ship

Fig. 3 shows the wall Y+ values for the smooth plate at three Reynolds numbers. The wall Y+ values are maintained same for all rough condition simulations. Prism layer and prism layer thickness study is carried out for the most fouled condition (heavy calcareous fouling); thus, the prism layer is fixed with appropriate prism layer thickness. For this case, the length of ship is large and so the Y+ value. Prism layer is fixed at 8 having less percentage error of 0.2%. Prism layer thickness at 0.8m were also carried

out in the heavy calcareous fouling with error of 0.001%. The prism layer thickness and prism layer requirement are validated on flat plate and tanker ship. From the validation, it is understood that Y+ value will reduce when the number of prism layer increases.

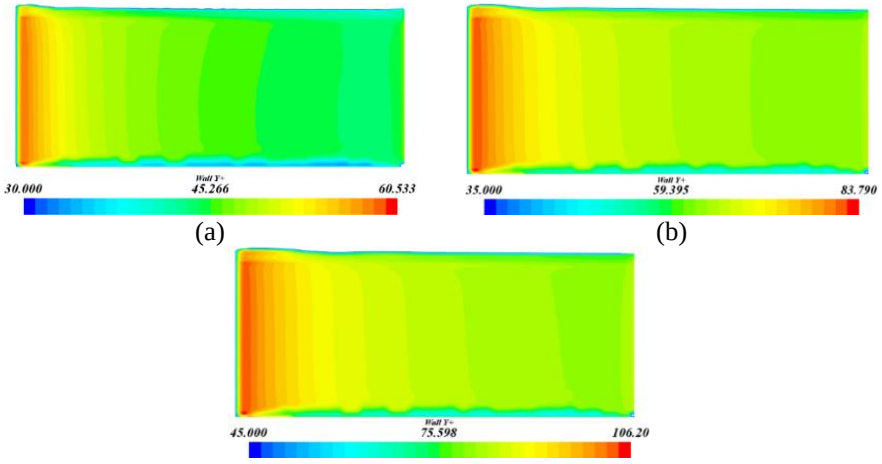

(a) (b)

(c)

Fig. 3. Wall Y+ values on the smooth plate at (a) Re=2.8x10^6, (b) Re=4.2x10^6, (c) Re=5.5x10^6

3 RESULTS AND DISCUSSION

3.1 Estimation of Frictional Resistance

Flat plate frictional coefficients are computed and compared with experiments for smooth, sandpaper and five different coatings such as silicon 1, silicon 2, ablative copper, SPC copper and SPC TBT at Re=2.8x10^6, Re=4.2x10^6 and Re=5.5x10^6 respectively. For all cases, the comparison of friction coefficient values using CFD is well matched with the EFD results, and the error percentage ranges from 0.37%-1.58%, See Fig. 4 As the roughness amplitude increases, the C_F values also increases but decreases with the increase in Reynolds's number.

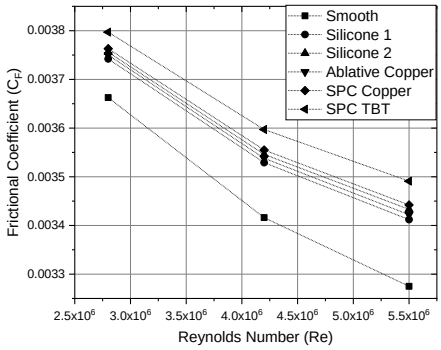

Fig. 4. Frictional resistance coefficient versus Reynolds number for antifouling coatings

The effect of roughness and Reynolds number is captured clearly by the CFD solver. Table.1 shows the results for 60-grit Sandpaper, where the roughness amplitude is almost 10 times than other cases.

Table 1. Comparison of C_F for 60-grit Sandpaper case

Reynolds Number (Re)	C_F (CFD)	C_F (EFD)	Error %
$2.8x10^6$	0.006150	0.006048	1.66%
$4.2x10^6$	0.006121	0.005941	2.94%
$5.5x10^6$	0.006124	0.005949	2.86%

The same computational setup and roughness conditions are used to generate and analyze the sandpaper roughness for the plate, and hence it is observed that the error percentage is slightly more than all other rough cases.

3.2 Estimation of Roughness Condition

To estimate the roughness parameters, the Reynolds roughness number, $k+$ is calculated using the experimental C_F values [12]. Computation of k^+ values is important to implement Schultz roughness function model, which provides the required ΔU^+ based on computed k^+ value shown [8]. The $k+$ distribution on the surface of the plate obtained from the CFD is verified with the calculated values. The k+ distribution on the plate with the SPC TBT coating and the comparison of the roughness height (k) with experimental data is shown in Fig. 5 and Fig. 6 respectively.

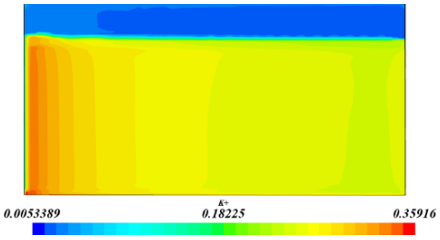

(a)

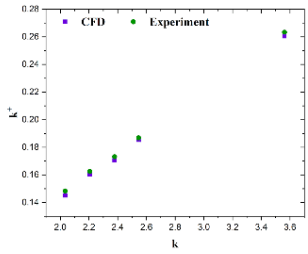

(a)

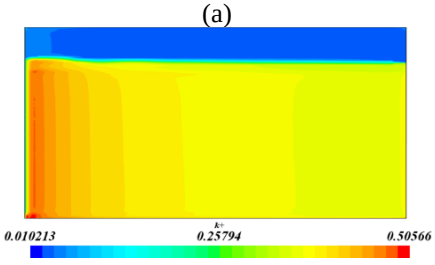

(b)

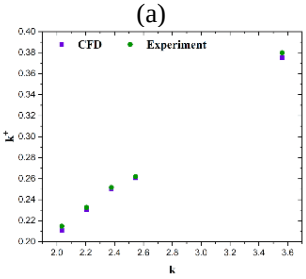

(b)

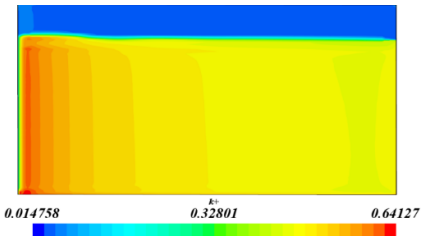

(c)

Fig. 5. k+ distribution on the plate coated with SPC TBT at (a) Re=2.8x10^6, (b) Re=4.2x10^6, (c) Re=5.5x10^6

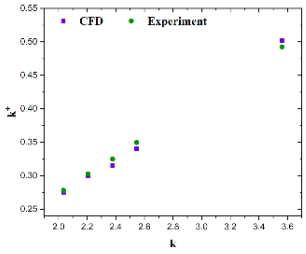

(c)

Fig. 6. Comparison of k with k+ at (a) Re=2.8x10^6, (b) Re=4.2x10^6, (c) Re=5.5x10^6

The frictional resistance coefficients (C_F) for the tanker are obtained for six different surface conditions over 12 knots, 15.5 knots and 18 knots ship speeds respectively. The frictional resistance coefficient of the full-scale tanker model is therefore predicted as 0.003518. Frictional resistance coefficients computed by CFD and obtained using the "ITTC 1957 model-ship correlation line", at a ship speed of 15.5 knots are well matched with difference ~0.09%. This CFD approach can therefore be claimed to be validated and can be used for further investigations. The predicted C_F values are reasonably reliable and consistent with those obtained using the similarity law scaling procedure [14]. The illustrative comparison of the C_F values with Granville similarity are shown in Fig.7 and Fig.8 respectively, the error between Granville and CFD are within limits.

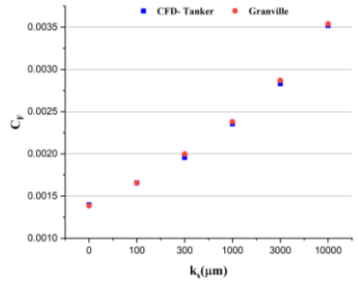

(a)

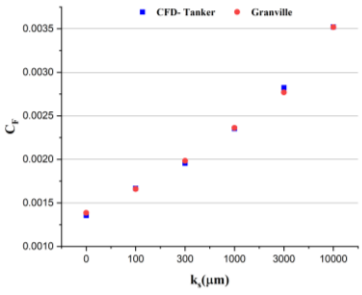

(b)

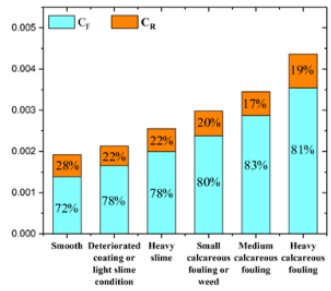

(a)

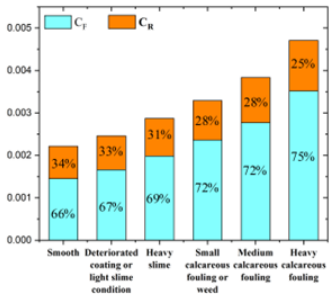

(b)

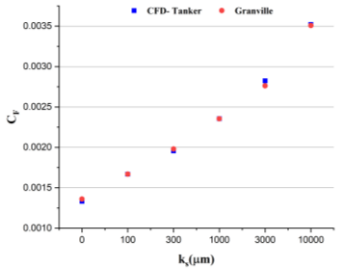

(c)

Fig. 7. Comparison of the C_F values of the tanker for different hull fouling conditions (a). 12 knots, (b). 15.5 knots, (c). 18 knots

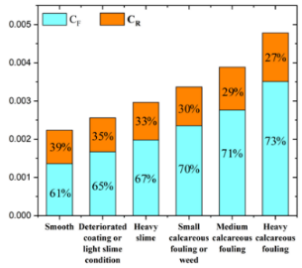

(c)

Fig. 8. Total resistance components C_F and C_R values at full scale (a). 12 knots, (b). 15.5 knots, (c). 18 knots

The ship speeds 12 knots and 18 knots are compared for the increase in effective power. With the increase in the fouling rate, the effective power increases and hence the heavy calcareous fouling is more vulnerable against other cases, See Fig.9. However, the comparison between the ship speeds shows that, sailing ate slow speeds require more power in the fouled conditions, See Fig.10.

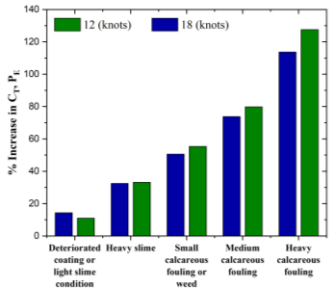

Fig. 9. Effective power of the KVLCC2 due to different surface conditions at 12 and 18 knots

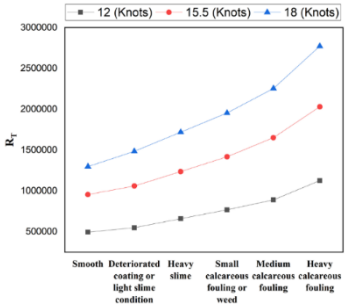

Fig. 10. Resistance of KVLCC2 due to different surface conditions at 12, 15.5 and 18 knots

4. CONCLUSION

This paper discusses the CFD analysis on a flat plate and a tanker to estimate the roughness effect due to different anti-fouling coatings and bio-fouling stages. The roughness condition estimation for the flat plate is compared with Colebrook-type roughness function. The results obtained are well matched with the experiments with an error percentage between 0.12% to 3.00%. The variation in the percentage difference may be due to implementing the same roughness parameters for all cases. The simulation with the flat plate is further extended to a tanker ship, where the hull is considered as a flat plate for evaluating the frictional component. The biofouling stages are modelled in the tanker hull to investigate the frictional resistance (C_F) as per the Schultz roughness functions. The frictional resistance of the ship at various speeds are compared with the ITTC 1957 rule. The simulation results of the frictional coefficient of the tanker is compared with Granville, the results shows a good agreement with the CFD and the literature. The effects of biofouling on the vessel's effective power are evaluated and analyzed. For

deteriorated condition, the increase in effective power is not significant however, at heavy calcareous condition this increase is recorded almost ten times greater and affects severely on the vessel's efficiency. With the latest amendments proposed by the IMO on ship's energy efficiency, the significant variation in the fouling rate is alarming. The methodology and the validation procedure used in this current study would further assist to estimate the higher fuel consumption rate and GHG emissions due to the marine growth on submerged hull.

5. References

1. IMO.: Annex 5, Resolution MEPC.245 (66), 2014 Guidelines on the method of calculation of the attained Energy Efficiency Design Index (EEDI) for new ships (2014).
2. IMO.: Annex 9, Resolution MEPC.213 (63), 2012 Guidelines for the development of a Ship Energy Efficiency Management Plan (SEEMP) (2012).
3. IMO.: MEPC 59/4/15, Prevention of air pollution from ships, Energy Efficiency Operational Indicator (EEOI) (2009).
4. ITTC.: The Specialist Committee on Energy Saving Methods, Final Report and Recommendations to the 28 th ITTC (2017).
5. Lackenby, H.: Resistance of ships with special reference to skin friction and hull surface condition, The 34th Thomas Lowe Grey Lecture, Proceedings of the Institute of Mechanical Engineers, Vol. 176, pp. 981-1014, (1962).
6. Schultz, M. P. & Swain, G.: The effect of biofilms on turbulent boundary layers. Journal of Fluids Engineering, 121, 44-51, (1999).
7. Taylan, M.: An overview: effect of roughness and coatings on ship resistance. International Conference on Ship Drag Reduction SMOOTH-SHIPS, (2010).
8. Schultz, M. P.: Effects of coating roughness and biofouling on ship resistance and powering. Biofouling, 23, 331-341, (2007).
9. Schultz MP.: Frictional Resistance of Antifouling Coating Systems, [DOI:10.1115/1.1845552], (2004).
10. Grigson, C.: Drag losses of new ships caused by hull finish. Journal of Ship Research, 36, 182-196, (1992).
11. Anthony F. Molland, Stephen R. Turnock, Dominic A. Hudson.: Ship Resistance and Propulsion, (2011).
12. Demirel Y K, Khorasanchi M, Turan O, Incecik A Schultz MP.: A CFD model for the frictional resistance prediction of antifouling coatings, (2014).
13. Granville, P. S.: Mixing-length formulations for turbulent boundary layers over arbitrarily rough surfaces. Journal of Ship Research, 29, 223-233, (1985).
14. Granville, P. S.: Three indirect methods for the drag characterization of arbitrarily rough surfaces on flat plates. Journal of Ship Research, 31, 70-77, (1987).
15. Granville, P. S.: The frictional resistance and turbulent boundary layer of rough surfaces. Journal of ship research, 2, 52-74, (1958).
16. Celik, I. B., Ghia, U., Roache, P. J., Freitas, C. J., Coleman, H. & Raad, P. E.: Procedure for estimation and reporting of uncertainty due to discretization in CFD applications. Journal of Fluids Engineering-Transactions of the ASME, 130, 078001-1-4, (2008).
17. Nikuradse, J.: Laws of flow in rough pipes, NACA Technical Memorandum 1292, (1933).
18. Yigit Kemal Demirel, Osman Turan, Atilla Incecik.: Predicting the effect of biofouling on ship resistance using CFD, Applied Ocean Research 62 (2017) 100–118, (2017).
19. SIMMAN2020, https://www.simman2020.kr/